Water Resources Research

RESEARCH ARTICLE
10.1029/2018WR023229

Key Points:
- Snow droughts can be classified as dry, warm, or warm and dry, based on winter precipitation and thawing degrees
- In many locations, temperature plays an important role in snow drought severity and risk
- The relationship between mean winter temperature and warm snow drought risk is nonlinear

Supporting Information:
- Supporting Information S1

Correspondence to:
J. R. Dierauer,
jen.r.brand@gmail.com

Citation:
Dierauer, J. R., Allen, D. M., & Whitfield, P. H. (2019). Snow drought risk and susceptibility in the western United States and southwestern Canada. *Water Resources Research*, *55*. https://doi.org/10.1029/2018WR023229

Received 30 APR 2018
Accepted 18 MAR 2019
Accepted article online 28 MAR 2019

Snow Drought Risk and Susceptibility in the Western United States and Southwestern Canada

Jennifer R. Dierauer[1], Diana M. Allen[1], and Paul H. Whitfield[1,2,3]

[1]Department of Earth Sciences, Simon Fraser University, Burnaby, British Columbia, Canada, [2]Centre for Hydrology, University of Saskatchewan, Saskatoon, Saskatchewan, Canada, [3]Environment and Climate Change Canada, Vancouver, British Columbia, Canada

Abstract In western North America (WNA), mountain snowpack supplies much of the water used for irrigation, municipal, and industrial uses. Thus, snow droughts (a lack of snow accumulation in winter) can have drastic ecological and socioeconomic impacts. In this study, the historical (1951–2013) frequency, severity, and risk (frequency × severity) of dry, warm, and warm and dry snow droughts are quantified at the grid-cell and ecoregion scale for snow-dominated regions in the western United States and southwestern Canada (sWNA). Based on multiple linear regression analysis, relationships between mean winter temperature, snow drought risk, and snow water equivalent sensitivity are explored. Piecewise linear regression is used to identify temperature thresholds for mapping temperature-related snow drought susceptibility. Results highlight spatial differences in snow drought regimes across sWNA and reveal that temperature thresholds exist at −3.1 °C (±0.3 °C) and 1.4 °C (±0.3 °C), above which the warm snow drought risk increases more rapidly. Approximately 3% of the nonglaciated snow storage in this region has high susceptibility to temperature-related snow drought, representing 11 km^3 of water, or approximately one third the capacity of Lake Mead. Under a +2 °C climate scenario, an additional 8% (28 km^3) of this snow storage volume will transition to high susceptibility.

Plain Language Summary In western North America, mountain snowpack fills reservoirs for agricultural, municipal, and industrial uses and sustains streamflow in summer when ecosystem needs are high. Thus, snow droughts (a lack of snow accumulation in winter) can have large social, economic, and environmental impacts. An analysis of the frequency and severity of past snow droughts shows that warm and dry winter conditions occurring together produce the most severe snow droughts, while warm winter conditions alone produce the least severe snow droughts. The severity and frequency of warm snow droughts, however, is dependent on mean winter temperature, and the risk of warm snow droughts is substantially higher for locations with mean winter temperatures above −3.1 °C (±0.3 °C). Approximately 3% of the volume of the western United States' and southwestern Canada's nonglaciated snowpack is highly susceptible to warm snow droughts, and an additional 24% exhibits medium susceptibility.

1. Introduction

In western North America (WNA), much of the water used for agriculture and human consumption comes from snow. The winter snow accumulation provides natural storage, with the following spring and summer snowmelt filling reservoirs and sustaining streamflow when precipitation is low and evapotranspiration rates are high. Compared to rainwater, snowmelt more effectively infiltrates below the root zone (Earman et al., 2006), and snowmelt often comprises a large fraction of groundwater recharge (Ajami et al., 2012; Earman et al., 2006; Winograd et al., 1998). Thus, snow drought, that is, a lack of snow accumulation in winter (Ludlum, 1978; Wiesnet, 1981), can have drastic ecological and socioeconomic impacts. For example, the 1 April snowpack in 2015 in the Pacific Northwest was 50% of normal, and snowpack in the Sierra Nevada—a key water source for much of California—was even lower, at only 5% of normal on 1 April 2015 (Harpold et al., 2017). California's agricultural economy depends on snowpack for water supply, and the 2015 drought resulted in an estimated $1.84 billion in agricultural losses (Howitt et al., 2015).

While both regions (Pacific Northwest and Sierra Nevada) exhibited below normal 2015 snowpack, the Pacific Northwest received near-normal precipitation (70–120%), while the Sierra Nevada received only 40–80% of the normal precipitation (Harpold et al., 2017). Mote et al. (2016) showed that exceptionally warm winter conditions prevented snow accumulation in the states of California, Oregon, and Washington during

the record low snow season of 2015, and Harpold et al. (2017) labeled the 2015 drought as a *warm snow drought* in the Pacific Northwest and a *dry snow drought* in the Sierra Nevada. While both snow drought types are defined by a lack of snow accumulation in winter, they have distinctly different climatic causes. Dry snow droughts are caused by winter precipitation deficits, while warm snow droughts are caused by above-normal winter temperatures, leading to late snow season onset, midseason melt or rain events, and/or early spring melt.

Due to the difference in climatic causes, these two different snow drought types have different hydrologic and socioeconomic impacts. Warm snow droughts reduce the annual flood peak due to increased rain versus snow proportion and a lengthening of the melt interval before the peak flow (Rood et al., 2016) and also increase flood risk due to rain on snow events (Allamano et al., 2009; Harpold et al., 2017; Rood et al., 2016). Hatchett and McEvoy (2018) showed that in Sierra Nevada watersheds, warm snow droughts correspond to lower snow fractions and often include midwinter flood events. Considering no change in the seasonal timing and magnitude of precipitation, warm snow droughts and the associated lower snow fractions lead to decreased annual runoff (Alexander et al., 2011; Berghuijs et al., 2014; Dierauer et al., 2018) and a shift in water supply away from summer and toward winter (Leith & Whitfield, 1998; see also Adam et al., 2009; Alexander et al., 2011; Déry et al., 2009; Pederson et al., 2011; Whitfield & Cannon, 2000, among others), negatively impacting water quantity, water quality, hydropower operations, winter snow sports, and summer recreation (Alexander et al., 2011; Sproles et al., 2017). Earlier snow disappearance has also been tied to increased wildfire activity (Westerling et al., 2006), increased tree mortality (Bales et al., 2018), greater water stress for mountain ecosystems (Harpold, 2016), and decreased carbon uptake (Hu et al., 2010; Winchell et al., 2016).

Unlike warm snow droughts, which often correspond to increased winter streamflow (Dierauer et al., 2018), dry snow droughts reduce streamflow year round (Dierauer et al., 2018; Harpold et al., 2017). Impacts from dry snow droughts include low reservoir levels, reduced hydropower production, and, in severe cases, drinking and irrigation water supply shortages. Both warm snow droughts and dry snow droughts cause below-normal summer streamflow (Dierauer et al., 2018; Harpold et al., 2017). Warm and dry winter conditions occurring together cause the most severe snow droughts and, consequently, the most severe summer streamflow drought conditions (Dierauer et al., 2018).

The predominance of warm versus dry snow drought is likely related to climate controls on the interannual variability of snow water equivalent (SWE). In cold, continental regions, the interannual variability of SWE is dominantly controlled by precipitation variability (Cline, 1997; Male & Granger, 1981). In maritime regions, however, the interannual variability of SWE is often dominantly controlled by temperature variability (Cooper et al., 2016; Harpold et al., 2012; Harpold & Kohler, 2017). These regional differences are related not only to large-scale modes of natural climate variability, like the El Niño–Southern Oscillation (Cayan et al., 1999; Fleming et al., 2007) and the Arctic Oscillation and Pacific-North American teleconnection (Guan et al., 2013) but also to regional climatology. Regions with winter and spring temperatures near 0 °C, like the Pacific Northwest, are particularly sensitive to climate warming (Adam et al., 2009; Brown & Mote, 2009; Luce et al., 2014).

In addition to regional differences, elevation plays a role in the precipitation-sensitivity (*P*-sensitivity) versus temperature-sensitivity (*T*-sensitivity) of SWE. Recent studies (Morán-Tejeda et al., 2013; Scalzitti et al., 2016; Sospedra-Alfonso et al., 2015) have shown that elevation thresholds exist above which SWE is temperature-dominated (*T*-dominated) and below which SWE is precipitation-dominated (*P*-dominated). The presence of these elevation thresholds is also evident in temporal trend studies, which have documented little to no change in SWE at high elevations (Mote, 2006; Mote et al., 2005) and large decreases at low elevations (Barnett et al., 2008; Groisman et al., 2004; Kapnick & Hall, 2012; Mote et al., 2005, 2018; Regonda et al., 2005).

Given the documented regional differences in SWE sensitivity and the existence of elevation thresholds between *T*-dominated and *P*-dominated areas, the predominance of dry versus warm snow drought likely varies between ecoregions and with temperature/elevation. Further, regions with higher peak SWE *T*-sensitivity likely exhibit greater risk to warm snow drought. Continued climate warming is expected to lead to reductions in peak SWE (Barnett et al., 2005, 2008; Brown & Mote, 2009; Seager et al., 2013), which will lead to corresponding shifts in snow drought regimes. Since different snow drought types have different

impacts and thus require different preparation measures and mitigation strategies, understanding the historical and potential future frequency and severity of these events is critical for managing water resources in WNA.

The ecological and socioeconomic impacts of changing snow hydrology in WNA are complicated and nonlinear (Hatcher & Jones, 2013; Jaeger et al., 2017), and while much research on this topic has been completed, results are often not easily transferrable or implemented into practice. Nolin and Daly (2006) mapped at-risk snow in the Pacific Northwest, but no other regional assessments of snow drought risk have been completed. Therefore, the overarching goal of this study was to complete a high-level assessment of snow drought risk in WNA in the context of a warming climate by meeting the following objectives: (1) develop a methodology for the classification of snow droughts based on climatic causes; (2) quantify the historical frequency, severity, and risk of snow drought at the grid cell and ecoregion scale; and (3) develop a method for snow drought susceptibility mapping. Results of this study highlight spatial and ecoregion differences in snow drought regimes across WNA and reveal that temperature thresholds exist, above which risk of temperature-related (i.e., warm) snow drought increases more rapidly. Further, the susceptibility mapping presented in this study highlights regions where the natural snow storage is likely to exhibit the largest negative impacts from continued climate warming.

The remainder of this paper is organized as follows. Section 2 presents the region of study and the data used and presents the methodology used to classify snow droughts and map snow drought susceptibility. The results are presented in section 3 and discussed in section 4. Conclusions are provided in section 5.

2. Materials and Methods

2.1. Data and Domain

Daily precipitation, mean daily temperature (calculated as the average between the minimum daily temperature and the maximum daily temperature), and daily SWE data used in this study were obtained from the Livneh et al. (2015) gridded hydrometeorological data set. This data set contains gridded observation-based daily meteorological forcings and simulated Variable Infiltration Capacity (VIC) model states and fluxes at 1/16° resolution (~30- to 40-km^2 grid cells) for the 1950 to 2013 period. The VIC model (Cherkauer et al., 2003; Liang et al., 1994) is a physically based land surface model capable of simulating energy and water balance. To account for the effects of topography, the Livneh et al. (2015) data set used a constant temperature lapse rate of −6.5 °C/km and incorporated orographic scaling across the entire domain, thereby providing a better representation of precipitation and improving the accuracy of snow estimates in mountain areas (Livneh et al., 2013, 2015). The parameterization and validation of the VIC model are described in Livneh et al. (2013).

Improving simulated and observation-based gridded estimates of SWE is a major field of research (see, e.g., Snauffer et al., 2018; Painter et al., 2016), and, compared to the VIC model, more complex snow models exist. Feng et al. (2008) compared several snow models by validating them against observations and showed that VIC performs better than the complex Community Land Model, version 3 (Dai et al., 2003), and agrees well with the more complicated Snow Thermal Model (Jordan, 1991). Other gridded SWE products are also available, including data sets from NASA's Global Land Data Assimilation System (Rodell et al., 2004), the ERA-Interim/Land reanalysis product (Balsamo et al., 2015), and the observation-based GlobSnow (Pulliainen, 2006). The Livneh et al. (2015) data set was chosen over the other available data sets because of its finer spatial resolution and longer temporal coverage. Additionally, the use of the Livneh et al. (2015) data set is in line with several other recent studies focused on snow hydrology in sWNA (e.g., Barnhart et al., 2016; Li et al., 2017). The Livneh et al. (2015) data set, however, extends only to 53°N, thus limiting the northern extent of this study, hence the study area designation of sWNA.

To focus on the mountain and intermountain basins of sWNA where seasonal snow cover plays an important role in the hydrological cycle, the analysis domain was masked by excluding grid cells that (1) had minimal snow cover (<2-cm mean peak SWE [1951–2000]), (2) were located in the plains ecoregions east of the Canadian Rockies (Figure 1), or (3) had >10% glacial coverage based on the Randolph Glacier Inventory (RGI 6.0; Pfeffer et al., 2014; Randolph Glacier Inventory Consortium, 2017). The glacierized grid cells were excluded from the analysis because, compared to snow-dominated regions, glacierized regions exhibit a

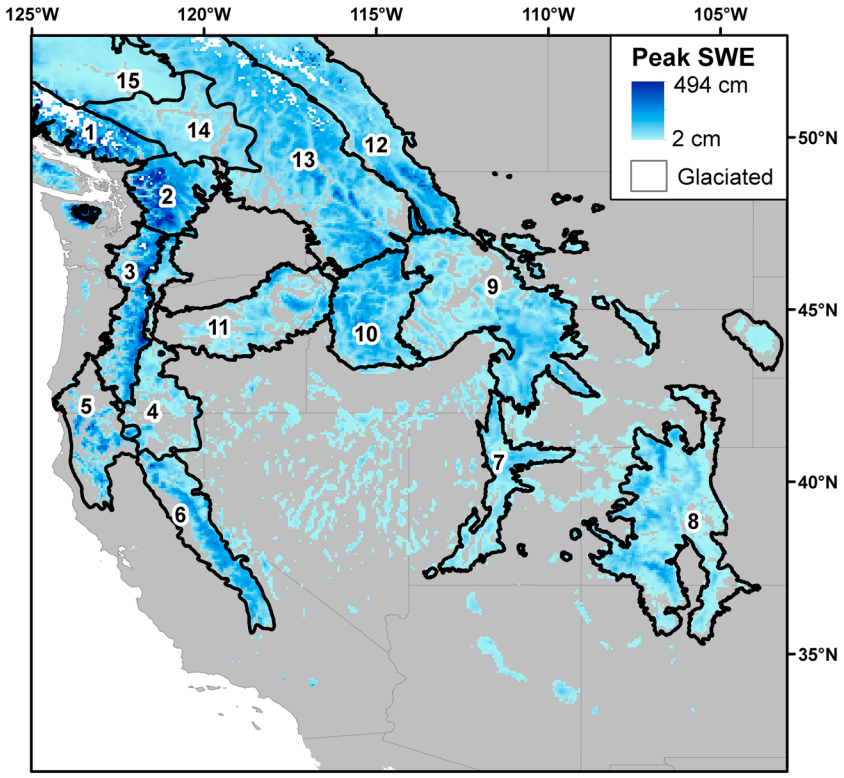

Figure 1. Ecoregions (Commission for Environmental Cooperation, 2011) and mean peak snow water equivalent (SWE; 1951–2000) for masked analysis domain. Ecoregions are outlined in black and include (1) Pacific and Nass Ranges, (2) North Cascades, (3) Cascades, (4) eastern Cascades slopes and foothills, (5) Klamath Mountains, (6) Sierra Nevada, (7) Wasatch and Uinta Mountains, (8) southern Rockies, (9) middle Rockies, (10) Idaho Batholith, (11) Blue Mountains, (12) Canadian Rockies, (13) Columbia Mountains/Northern Rockies, (14) Thompson-Okanagan Plateau, (15) Chilcotin ranges and Fraser Plateau. Grid cells with >10% glacial coverage based on the Randolph Glacier Inventory 6.0 (RGI Consortium, 2017) shown in white. SWE = snow water equivalent.

contrasting response to warmer temperatures, including summer flow augmentation (Moore et al., 2009; O'Neel et al., 2014), particularly in years with low-snow accumulation (Moore et al., 2009). The final masked area contained 32,073 VIC simulation grid cells covering an area of 1,083,654 km^2 (Figure 1). To aid in regional analysis, results were further summarized for the 15 level III ecoregions (Commission for Environmental Cooperation, 2011) with the greatest snow storage (Figure 1).

2.2. Snow Drought Classification

To separate warm snow droughts from dry snow droughts, a robust classification scheme is needed—one that works for a range of climate conditions. Harpold et al. (2017) suggest distinguishing warm versus dry snow droughts based on 1 April SWE and 1 November to 1 April cumulative precipitation, where winters with below-normal SWE and above-normal precipitation are classified as warm snow droughts and years with below-normal SWE and below-normal precipitation are classified as dry snow droughts. While the classification scheme proposed by Harpold et al. (2017) is straightforward and easy to use, it does not account for the co-occurrence of warm and dry conditions, which have been shown to result in significantly more severe summer low flow periods than only dry conditions alone (Dierauer et al., 2018). Additionally, it does not account for spatial and temporal variations in the timing of peak SWE, which varies substantially between and within mountain ranges (Wrzesien et al., 2018).

In this study, winters with below-normal peak SWE are classified as warm, dry, or warm and dry snow droughts based winter precipitation (P) and winter thawing degrees (TDs) using the following conditional statements:

$$if\left\{\left(\mathrm{SWE}_i<\overline{\mathrm{SWE}}\right)\&\left(P_i<\overline{P}\right)\&\left(\mathrm{TD}_i<\overline{\mathrm{TD}}\right)\right\}D_{\mathrm{type}}=\mathrm{DRY} \quad (1)$$

$$if\left\{\left(\mathrm{SWE}_i<\overline{\mathrm{SWE}}\right)\&\left(P_i>\overline{P}\right)\right\}D_{\mathrm{type}}=\mathrm{WARM} \quad (2)$$

$$if\left\{\left(\mathrm{SWE}_i<\overline{\mathrm{SWE}}\right)\&\left(P_i<\overline{P}\right)\&\left(\mathrm{TD}_i>\overline{\mathrm{TD}}\right)\right\}D_{\mathrm{type}}=\mathrm{WARM\&DRY} \quad (3)$$

where SWE_i, P_i, and TD_i are the peak SWE, winter precipitation, and winter thawing degrees in year i, respectively; $\overline{\mathrm{SWE}}$, $\overline{P}$, and $\overline{\mathrm{TD}}$, are the associated normals for the 1951–2000 period; and D_{type} is the snow drought type. Thawing degrees (TDs) were calculated as the sum of mean daily temperatures for all winter days with a mean daily temperature above 0 °C. Peak SWE was used (as opposed to 1 April SWE) because of the variability in the date of peak snowpack over the large and topographically complex region of sWNA. A 50-year reference period (1951–2000) was used to calculate the climate and peak SWE normals because it spans the range of natural climate variability while excluding the recent extremes.

Using $\overline{\mathrm{SWE}}$ as the threshold to define snow droughts results in the identification of many *minor* snow drought events, where winter season peak SWE levels are near normal. Thus, the frequency of snow droughts may be overestimated, especially in locations where the distribution of peak SWE is strongly right skewed. Warm snow droughts, which are of primary interest in this research, are likely to be relatively minor events; therefore, the use of high threshold was deemed appropriate, as a lower threshold would likely exclude many temperature-based SWE anomalies.

For the snow drought classification, a grid-cell-based definition of the winter season was used, where *winter* was defined based on the 25th percentile of the mean daily temperature (T_{25}). The use of the temperature criteria, T_{25}, provides a fairer comparison than an arbitrary calendar date and follows recommendations of Cannon (2005) to define seasons based on climatological data. With this method, the set of days with a T_{25} (1951–2000) less than 0 °C was defined as winter. The start of the winter season was then defined as the first day of the year occurring after the warmest day of the year with a T_{25} less than 0 °C. The grid-cell-based definition of the winter season is based on the climate of each individual grid cell and is applied in the same manner across the entire analysis domain.

To classify snow droughts, TD was used as the temperature metric, as opposed to mean winter temperature (T_{w}), because of the nonlinear response of SWE to T_{w}. For example, in regions with a normal T_{w} near 0 °C, a positive T_{w} anomaly will have a large influence on SWE, while a negative T_{w} anomaly may have minimal impact on SWE. This grid-cell-based approach using TD as a predictor variable is more complicated than the common 1 October/1 November to 1 April winter classification used in previous studies (e.g., Luce et al., 2014; Mote, 2003). A methodological comparison showed that a grid-cell-based winter definition with TD and P as predictor variables had the highest predictive ability for peak SWE (Table S2 in the supporting information). Additionally, the temperature metric (TD) had the highest regression slope (Table S3) and lowest standard error (Table S4) for the warmer maritime regions, where temperature is expected to play a large role in the snow drought regime.

After classifying each winter season with below-normal peak SWE as a warm, dry, or warm and dry snow drought, the severity, frequency, and risk of each snow drought type were calculated. Severity was calculated from normalized peak SWE as the fraction below the mean. Frequency was calculated as the fraction of total years ($n = 63$) exhibiting the associated snow drought type. The risk to each snow drought type was then calculated as the mean severity multiplied by the frequency and termed warm, dry, and warm and dry snow drought risk. Thus, risk has units of fractional deficit per year and is equal to the expected annual deficit in peak SWE for each drought type.

To quantify broad-scale spatial patterns in snow drought regimes, snow droughts were also classified and quantified at the ecoregion scale. For the ecoregion analysis, time series of average peak SWE, P, and TD were first calculated for each ecoregion as the average for all grid cells within the ecoregion. Snow drought classification and calculation of severity, frequency, and risk were then carried out in the same manner as the grid-cell-scale analysis. A lookup table of terms and abbreviations used in this paper is included in Table S1 for reference, and the methods used to calculate snow drought risk are included in equation form in Text S1.

2.3. Precipitation (*P*) Versus Temperature (*T*) Sensitivity

Risk of warm versus dry snow drought is likely related to the *T*- and *P*-sensitivity of peak SWE, with regions with higher peak SWE *T*-sensitivity exhibiting greater risk to warm snow drought. To test this hypothesis, peak SWE sensitivity was quantified using multiple linear regression (MLR) analysis. Variables were kept consistent with the snow drought classification, and the predictor variables (TD and *P*) were standardized by subtracting the mean and dividing by the standard deviation (SD). By using standardized values for the predictor variables, the MLR analysis produces regression coefficients that can be directly compared between predictor variables that have different nonstandardized units, for example, precipitation (cm) and thawing degrees (°C). The response variable, peak SWE, was normalized by dividing by the mean. By standardizing the predictor variables (TD and *P*) and normalizing the response variable (peak SWE), the MLR analysis produces regression coefficients that represent the percent change in SWE for every 1 SD change in the predictor variables, thus providing a measure of the *T*-sensitivity and *P*-sensitivity of peak SWE that can be directly compared between grid cells.

2.4. Temperature Thresholds and SWE Susceptibility Mapping

Because of the nonlinear relationship between temperature and snowpack, a temperature threshold likely exists, above which *T*-sensitivity and warm snow drought risk increase sharply. To objectively identify such temperature thresholds, piecewise linear regression was implemented with the R package *segmented* (Muggeo, 2008). Piecewise linear regression is a regression method where the independent variable is divided into segments and the regression analysis is performed separately for each segment. The boundaries between the segments are termed breakpoints. In piecewise linear regression, the resulting regression equations exhibit no discontinuity at the breakpoints (Seber, 2015). In this study, the 1951–2000 normal mean winter (1 November to 1 April) temperature (T_w) was used as the predictor (independent) variable, with warm, dry, and warm and dry, snow drought risk and peak SWE *T*- and *P*-sensitivity as the response (dependent) variables. T_w, as opposed to TD, was used as the predictor because it is more easily calculated and requires only widely available climate data, thus allowing for the potential transfer of this methodology to other places. Based on visual assessment of the scatterplots, piecewise regression models with two breakpoints and a lower cutoff temperature at −10 °C were investigated. The existence of breakpoints, and significant differences in slope between regression segments, was tested using the Davies's test (Davies, 1987). Final models were chosen based on the R^2 values and the standard error of the piecewise regression slopes (magnitude less than corresponding slope). The 95% confidence intervals for the breakpoints were estimated with bootstrap resampling, using 1,000 samples with replacement.

Based on the breakpoints, or *thresholds*, identified from this analysis, the susceptibility of peak SWE to temperature-related snow drought was ranked as negligible, low, medium, or high. This classification was completed at the grid-cell scale using the following T_w ranges:

$$\text{Negligible}: \quad T_w \leq -10^{\circ}C \tag{4}$$

$$\text{Low}: \quad -10^{\circ}C < T_w \leq \text{BP}_1 \tag{5}$$

$$\text{Medium}: \quad \text{BP}_1 < T_w \leq \text{BP}_2 \tag{6}$$

$$\text{High}: \quad T_w > \text{BP}_2 \tag{7}$$

where BP_1 is the dominant breakpoint separating regression segments 1 and 2 and BP_2 is the dominant breakpoint separating regression segments 2 and 3. This T_w threshold approach allows for the evaluation of temperature-related snow drought susceptibility under simple climate warming scenarios. For example, in this study, the impact of a +2 °C climate scenario on the temperature-related snow drought susceptibility was quantified by subtracting 2 °C from each of the breakpoints and the lower cutoff temperature and reclassifying the grid cells.

3. Results

Figure 2 shows the spatial variation of snow drought frequency, severity, and risk, and Figure 3 shows the snow drought regimes for the major mountainous ecoregions in sWNA. Substantial spatial variation exists

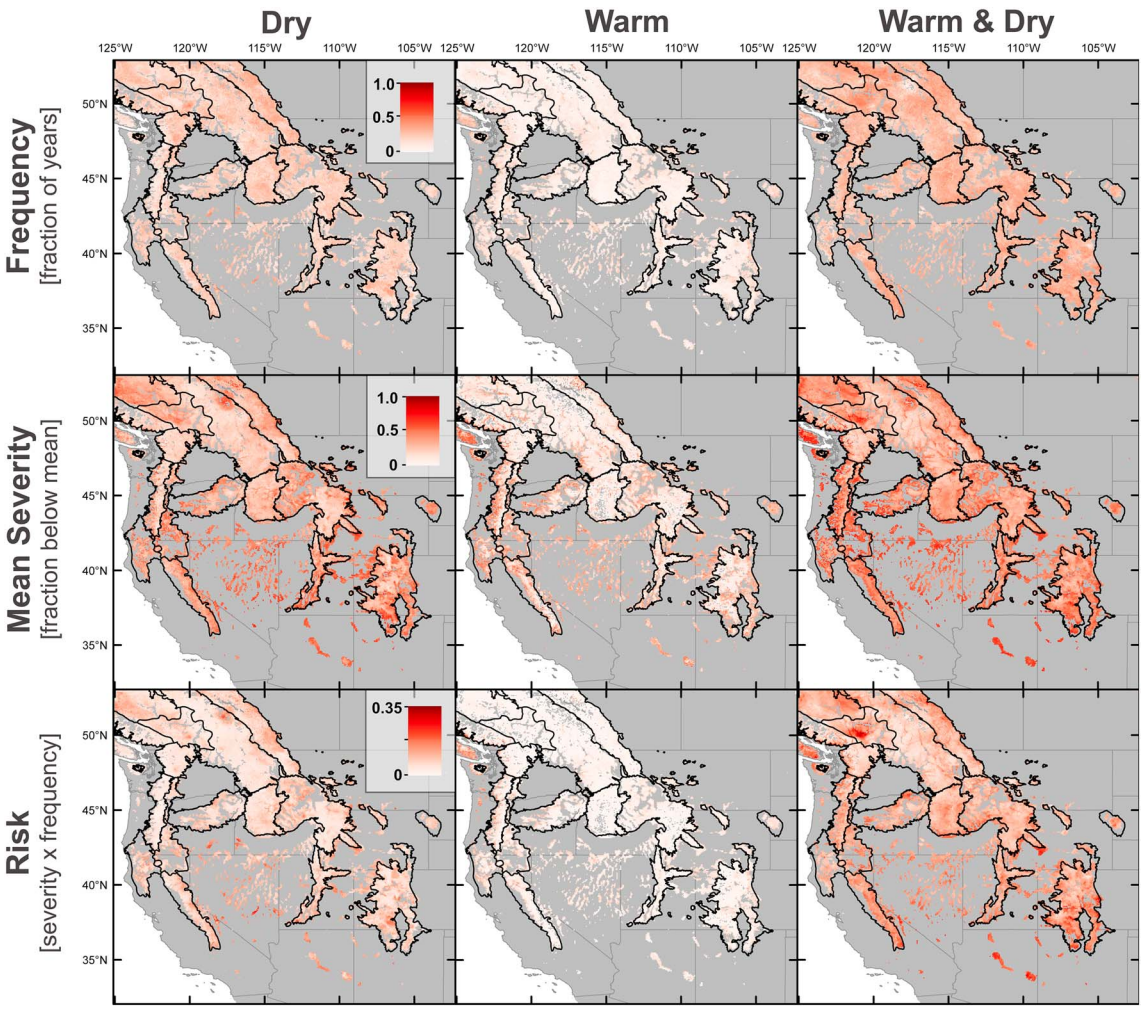

Figure 2. Frequency, severity, and risk for dry, warm, and warm and dry snow droughts, 1951–2013. See Figure S1 for alternative version with major watersheds delineated.

both between and within ecoregions. Dry, and warm and dry, snow droughts occur throughout the entire analysis domain, while warm snow droughts have a more limited spatial occurrence (Figure 2). Warm snow droughts do not occur at some high elevation locations and tend to be more frequent and severe at lower elevations. Similarly, warm and dry snow droughts tend to have higher severity at lower elevations (Figure 2).

Overall, warm snow drought is the least frequent and least severe of the three snow drought types and thus exhibits the least risk. Warm snow droughts are most frequent in the Cascades, Pacific and Nass Ranges, and the Klamath Mountains; least frequent in the Thompson-Okanagan Plateau and the Chilcotin Ranges and Fraser Plateau; and most severe in the Klamath Mountains. Warm and dry winter conditions occurring together correspond to the most severe snow drought type. Warm and dry snow droughts are also the most frequent drought type in 11 of the 15 ecoregions, with dry snow drought dominating the Pacific and Nass Ranges, Klamath Mountains, Middle Rockies, and Canadian Rockies. Warm and dry snow droughts exhibit the highest risk of the three drought types in all ecoregions except the Klamath Mountains, where dry snow drought risk is highest, and the Pacific and Nass Ranges and Canadian Rockies, where dry snow drought risk and warm and dry snow drought risk are approximately equal (Figure 3 and Table S5). Excluding the Klamath Mountains, warm and dry snow drought risk increases southward along the coastal mountain ranges (Figure 3), and, compared to the other ecoregions, warm and dry snow drought risk is substantially higher in Sierra Nevada, where the expected annual peak SWE deficit is 14%/year.

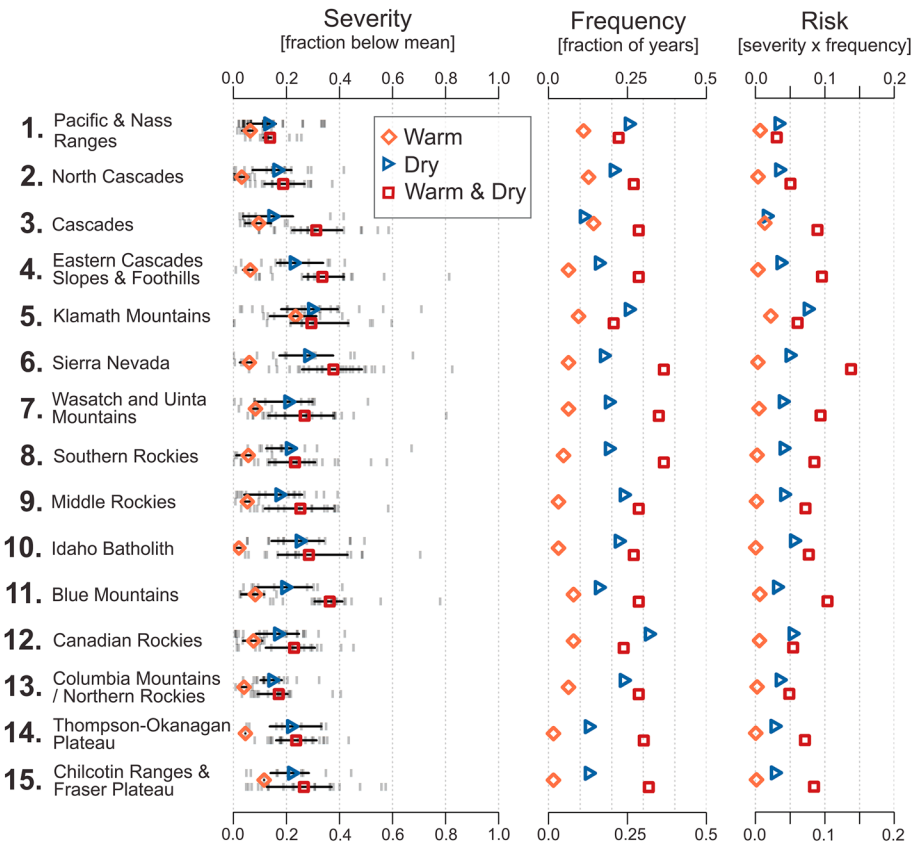

Figure 3. Snow drought severity, frequency, and risk by ecoregion, 1951–2013. For severity, the gray vertical lines represent individual years, the black horizontal lines span the interquartile range, and the symbols coincide with the mean. Ecoregion numbering as in Figure 1. See Table S5 for values of mean severity, frequency, and risk in table format.

While Figures 2 and 3 highlight the large spatial and ecoregion differences in snow drought risk, plots of snow drought risk and peak SWE T- and P-sensitivity versus T_w (Figure 4) reveal that temperature controls warm snow drought risk and peak SWE T-sensitivity in sWNA. Moreover, warm snow drought risk exhibits a strong positive correlation ($r = 0.89$, $p < 0.01$) with peak SWE T-sensitivity, confirming the hypothesis that regions with higher peak SWE T-sensitivity exhibit greater risk to warm snow drought. Both warm snow drought risk and peak SWE T-sensitivity tend to be higher at lower elevations, as illustrated in Figures 2 and S2, respectively. Dry snow drought risk, on the other hand, exhibits no substantial correlation with T-sensitivity but is strongly correlated ($r = 0.69$, $p < 0.01$) with P-sensitivity, and regions with higher P-sensitivity exhibit greater risk to dry snow drought. As expected from these relationships, and shown in Figures 4b and 4d, warm snow drought risk and T-sensitivity are strongly correlated with T_w, while dry snow drought risk and P-sensitivity exhibit no substantial correlation with T_w. Warm and dry snow drought risk is related to both precipitation and temperature and exhibits a weak correlation with T_w (Figure 4c).

T_w has a nonlinear relationship with both warm snow drought risk and T-sensitivity (Figures 4b and 4d). Piecewise linear regression analysis confirms the presence of temperature thresholds, above which T-sensitivity and warm snow drought risk increase sharply (Figures 4b and 4d). Linear regression slopes increase substantially at the identified breakpoints, increasing from 0.2%/°C to 3.8%/°C for warm snow drought risk and from 1.6%/°C to 11.7%/°C for T-sensitivity at the low (S1) and high slopes (S3), respectively (Figures 4b and 4d). Warm snow drought risk and T-sensitivity have breakpoints located at −3.1 °C (95% CI [−2.8, −3.3]) and −2.4 °C (95% CI [−2.5, −2.2]), respectively. Warm snow drought risk and T-sensitivity also have a second breakpoint located at 1.4 °C (95% CI [1.1, 1.5] and [0.76, 1.6], respectively) showing that increasing temperatures can be expected to have larger negative impacts on SWE in locations where the T_w is greater than −3.1 °C, and even larger negative impacts in locations where T_w is greater than 1.4 °C.

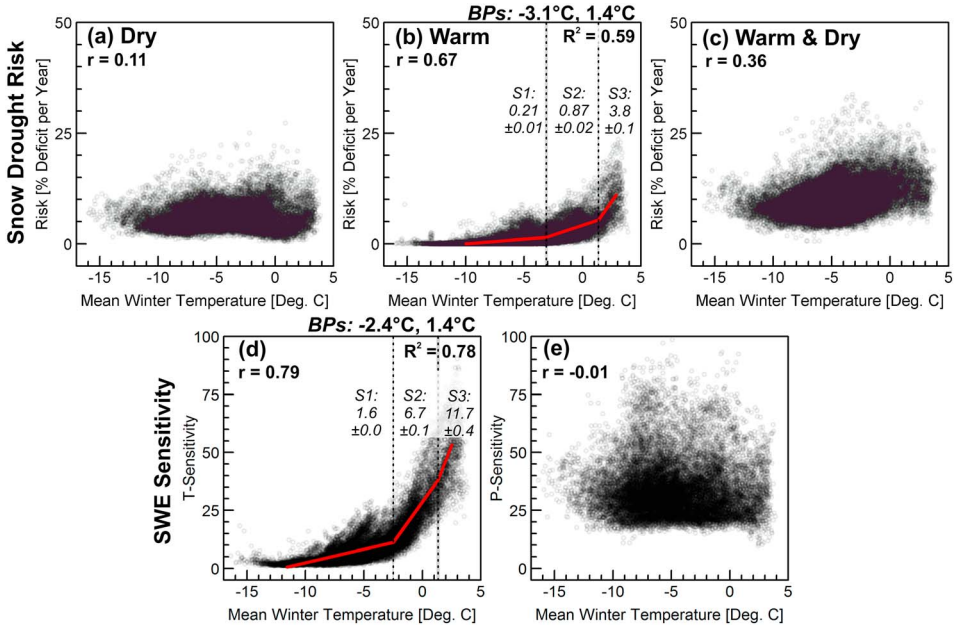

Figure 4. Snow drought risk and peak SWE sensitivities versus the 1951–2000 normal mean winter (1 November to 1 April) temperature [T_w]. Top row: Snow drought risk from (a) dry, (b) warm, and (c) warm and dry snow drought events. Bottom row: Peak SWE sensitivity to (d) temperature and (e) precipitation. Piecewise linear regression lines are shown in red for variables with strong correlations with temperature (r values shown in top left corners). Breakpoints (BPs) from the piecewise regression are shown with black vertical dashed lines; gray shading behind breakpoint lines shows 95% confidence intervals. Slopes (S1, S2, and S3) and associated standard errors are indicated for each linear regression segment. Model performance indicated by coefficient of determination (R^2). See Figure S3 for plot (b) separated by ecoregion. SWE = snow water equivalent.

At the ecoregion scale, correlation coefficients between warm snow drought risk and T_w are consistently positive and tend to be higher in the warmer ecoregions (Figure S3). The nonlinear relationship between warm snow drought risk and T_w is evident in all ecoregions (Figure S3), and, for ecoregions with grid cells spanning more than one temperature range, that is, segments S1, S2, and S3 in Figure 4b, ecoregion-scale regression slopes increase by an order of magnitude greater than the associated standard errors (Figure S3 and Table S6). Based on the nonlinear relationship shown in the region-wide plot (Figure 4b) and the ecoregion plots (Figure S3), thresholds of −3.1 °C and 1.4 °C were chosen for the susceptibility mapping, corresponding to BP_1 and BP_2 in equations (4)–(6) (see section 2.4).

Peak SWE susceptibility to temperature-related snow drought is shown in Figure 5 and further summarized by ecoregion in Tables 1 and S7. The high-susceptibility category represents areas with the highest-temperature-related (i.e., warm and warm and dry) snow drought risk, highest peak SWE T-sensitivity, and the largest expected increases in risk per degree increase in T_w (i.e., S3 in Figures 4b and 4d). Conversely, the low-susceptibility category represents areas with the lowest-temperature-related snow drought risk, lowest peak SWE T-sensitivity, and the lowest expected increases in risk per degree increase in T_w (i.e., S1 in Figures 4b and 4d).

The Klamath Mountains exhibit the highest susceptibility to temperature-related snow drought, with 26% of the ecoregion's snow volume categorized as high susceptibility (Table 1). The Cascades and Sierra Nevada also have substantial susceptibility, with 8% and 9% of the snow volume classified as highly susceptible, respectively. The Middle Rockies, Canadian Rockies, and Chilcotin Ranges/Fraser Plateau, on the other hand, have the lowest susceptibility (Table 1). Overall, peak SWE is more susceptible to temperature-related snow droughts in the maritime ecoregions (ecoregions 1–6) and less susceptible in the continental ecoregions (ecoregions 7–15). In total, 3% of the nonglaciated snow storage volume in sWNA is highly susceptible to temperature-related snow droughts (Table 1), that is, 3% of the mean peak SWE volume within the analysis domain defined in section 2.1 and shown in Figure 1. This represents 11 km^3 of water, or approximately one third the capacity of Lake Mead. Under a +2 °C climate scenario, an additional 6% (24 km^3) of the sWNA

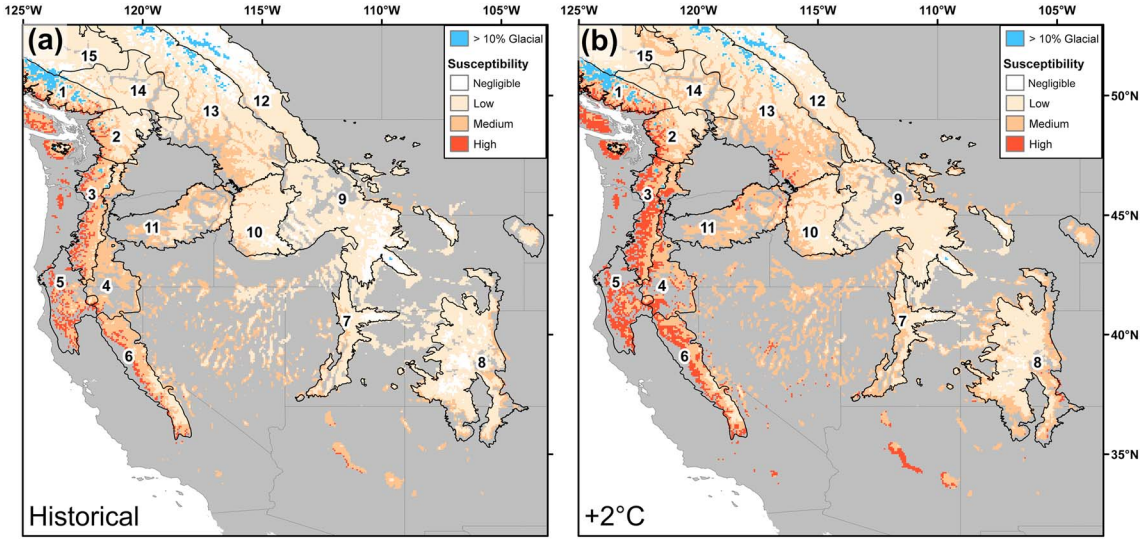

Figure 5. Peak snow water equivalent temperature-related snow drought susceptibility under (a) historical [1951–2000] and (b) +2 °C climate scenario. Ecoregion numbering as in Figure 1. Results are summarized by ecoregion in Tables 1 and S7.

snow storage volume will transition to high susceptibility, including an additional 33% and 26% of the snow storage volume in the Klamath Mountains and Cascades, respectively.

4. Discussion

Defining snow drought types by climatic causes is a relatively new concept (e.g., Harpold et al., 2017). While several recent studies have increased our understanding of snow drought (e.g., Cooper et al., 2016; Hatchett

Table 1
Temperature-Related Snow Drought Susceptibility Summarized by Ecoregion

		Historical				+2 °C warming			
	Vol.	Neg.	Low	Med	High	Neg.	Low	Med	High
Ecoregion	(km^3)	(% volume)				(% Change)			
1. Pacific and Nass Ranges	20.4	0%	58%	40%	2%	0%	−29%	+20%	+9%
2. North Cascades	32.5	3%	62%	34%	1%	−3%	−23%	+21%	+5%
3. Cascades	27.8	0%	20%	71%	9%	0%	−16%	−9%	+26%
4. Eastern Cascades Slopes and Foothills	9.2	0%	26%	72%	1%	0%	−21%	3%	+17%
5. Klamath Mountains	10.3	0%	5%	69%	26%	0%	−5%	−27%	+33%
6. Sierra Nevada	21.6	0%	34%	58%	8%	0%	−14%	−4%	+18%
7. Wasatch and Uinta Mountains	9.7	12%	81%	7%	0%	−7%	−13%	+20%	0%
8. Southern Rockies	27.2	26%	71%	3%	0%	−21%	+12%	+9%	0%
9. Middle Rockies	36.1	36%	64%	0%	0%	−28%	+25%	+4%	0%
10. Idaho Batholith	31.3	7%	89%	4%	0%	−6%	−7%	+13%	0%
11. Blue Mountains	11.5	0%	61%	39%	0%	0%	−36%	+34%	+1%
12. Canadian Rockies	36.4	39%	61%	0%	0%	−15%	+11%	+4%	0%
13. Columbia Mountains/N. Rockies	72.3	16%	71%	13%	0%	−13%	−6%	+19%	+1%
14. Thompson-Okanagan Plateau	14.4	10%	87%	3%	0%	−9%	−6%	+16%	0%
15. Chilcotin Ranges and Fraser Plateau	9.5	20%	80%	0%	0%	−14%	+5%	+9%	0%
Other	24.7	0%	44%	48%	9%	0%	−23%	+8%	+16%
Total	394.6	14%	60%	24%	3%	−9%	−7%	+10%	+6%

Note. Volume (vol.) refers to the mean volume of water stored as snow within the study domain, calculated by multiplying grid-cell mean peak SWE (1951–2000) by the corresponding grid-cell area then summing the result. Grid cells with >10% glacial coverage based on the Randolph Glacier Inventory 6.0 (RGI Consortium, 2017) and cells with less than 2-cm mean peak SWE [1951–2000] were excluded from the analysis domain (see section 2.1 and Figure 1); therefore, Vol. is an underestimate of the average volume of water stored as snow/ice in each ecoregion. Vol. = mean snowpack water volume; Neg. = Negligible. Ecoregion numbering as in Figure 1; SWE = snow water equivalent. "Other" includes all grid cells not within the 15 ecoregions. Table S7 presents the same data in terms of area as opposed to volume.

& McEvoy, 2018; Sproles et al., 2017), a regional assessment of snow drought risk has never before been completed. In this study, the dry versus warm snow drought definition proposed by Harpold et al. (2017) was expanded to include snow droughts that are caused by the co-occurrence of warm and dry conditions. A regional-scale analysis of historical snow drought severity, frequency, and risk showed that warm and dry snow droughts dominate the snow drought regime in sWNA, while warm snow droughts are the least common and least severe snow drought type. The severity and frequency of warm snow droughts, however, is dependent on T_w. Temperature thresholds identified with piecewise linear regression show that the risk of warm snow droughts is substantially higher for locations where T_w is above −3.1 °C and higher still for locations where the T_w is above 1.4 °C.

Spatial variation in snow drought risk is primarily driven by elevation, latitude, and proximity to the onshore flow of moisture. Warm snow drought risk, warm and dry snow drought risk, and *T*-sensitivity all exhibit significant positive correlations with T_w (Figure 4; see Table S1 for a lookup table of abbreviations), indicating that these metrics tend to decrease with increasing elevation. The relationship between snow drought risk and elevation, however, is also dependent on latitude, as isotherms increase in elevation as latitude decreases. The tendency for *T*-sensitivity to decrease with elevation and increase with temperature has been documented by many previous studies (e.g., Jenicek et al., 2016; Morán-Tejeda et al., 2013; Mote, 2006; Mote et al., 2005; Nolin & Daly, 2006; Safeeq et al., 2016; Sospedra-Alfonso et al., 2015; Sospedra-Alfonso & Merryfield, 2017); however, no previous studies have documented the interrelationships between *T*-sensitivity, T_w, and snow drought risk. Unlike warm, and warm and dry, snow drought risk, dry snow drought risk exhibits no substantial correlation with T_w and is instead dominantly controlled by the onshore flow of moisture. The leeward sides of mountain ranges tend to exhibit higher dry snow drought risk, especially for the interior plateaus of British Columbia and the Eastern Cascades (ecoregions 14, 15, and 4 in Figure 1 and Table 1). The spatial patterns in dry snow drought risk are consistent with precipitation pathways and anomaly patterns for WNA (e.g., Alexander et al., 2015; Sellers, 1968; Swales et al., 2016).

Snow drought risk in WNA has not been quantified at the regional scale before, nor has risk to any temperature-influenced drought type (e.g., agricultural, hydrologic, and socioeconomic) ever been quantified based on climatic causes. Verdon-Kidd and Kiem (2010) call for drought risk assessments that are derived from an understanding of the climate mechanisms that drive periods of elevated risk, pointing out that in a nonstationary climate, future drought risk may not resemble the past. Using the temperature thresholds, identified at T_w values of −3.1 and 1.4 °C, to complete the susceptibility mapping in this study identifies regions that (1) historically exhibit relatively high levels of temperature-related snow drought risk and (2) are likely to exhibit the largest negative impacts on peak SWE from continued climate warming. In the context of climate warming, the historical versus +2 °C susceptibility mapping (Figure 5 and Tables 1 and S7) can be used to identify regions where the snow drought regimes may shift toward more temperature-related snow droughts in the near future. Thus, the methodology presented in this study is a first step toward a regional snow drought risk assessment in the context of a nonstationary climate.

The temperature thresholds identified in this study differ from previous elevation/temperature thresholds (e.g., Morán-Tejeda et al., 2013; Sospedra-Alfonso et al., 2015; Sospedra-Alfonso & Merryfield, 2017) in that they do not separate *P*-dominated from *T*-dominated SWE regions, but rather identify breakpoints at which the relationship between T_w and peak SWE changes. As T_w increases, warm snow drought risk and *T*-sensitivity increase; however, the rate of increase is not constant. Once a temperature threshold is crossed, temperature-related decreases in peak SWE can be expected to *accelerate*, and a 1 °C increase in T_w has a larger negative impact on peak SWE for regions where T_w is above the temperature thresholds versus regions where T_w is below the temperature thresholds. The nonlinear relationship between temperature and SWE *T*-sensitivity is consistent with previous studies (Adam et al., 2009; Brown & Mote, 2009; Luce et al., 2014), which have shown that snow in warm locations where winter temperatures are near the rain-snow transition has higher *T*-sensitivity than snow in colder locations.

In the context of historical (1951–2000) climate conditions, warm snow drought impacts are likely to be most severe at lower elevations and in the Klamath Mountains ecoregion, where warm snow drought severity and frequency are high. In the context of climate warming, the maritime ecoregions (1–6 in Tables 1 and S7) will likely experience the largest increases warm snow drought risk and thus increased midwinter flood events, decreased annual runoff, and shifts in the seasonal timing of streamflow. This is consistent with the study by

Luce et al. (2014), which showed that snow in wet warm locations is more sensitive to temperature increases, and with the recent study by Mote et al. (2018), which showed that declines in western U.S. snowpack are largely temperature driven, with the largest downward trends in SWE in locations with mild, wet climates. With continued climate warming, dry snow droughts are likely to transition, in part, to warm and dry snow droughts, which cause significantly more severe summer low flow periods than only dry conditions alone (Dierauer et al., 2018), as well as overall reductions in annual runoff (Berghuijs et al., 2014; Dierauer et al., 2018). Regions with medium or high susceptibility to temperature-related snow drought along with relatively high risk to dry snow drought (i.e., Klamath Mountains and Sierra Nevada) are likely to have the largest risk to water quantity shortages in reservoirs and streams in the near future.

This study provided needed insight into the spatial and ecoregion differences in snow drought regimes across sWNA and developed the first regional assessment of snow drought risk in the context of a warming climate; however, this study has several limitations that should be addressed with future research. The primary limitation is that this study relied entirely on VIC-simulated SWE with a relatively coarse grid resolution. The use of only one model was deemed appropriate for analyzing regional patterns in snow drought risk and completing the high-level assessment of snow drought susceptibility presented in this study. Future research employing more complex snow models at higher spatial resolutions would likely reveal higher spatial heterogeneity and provide insight into how snow drought regimes and snow drought susceptibility/risk vary at the watershed scale due to vegetation, slope, aspect, etc. Additionally, further study with observed data, like the SWE time series available from the U.S. Natural Resource Conservation Service Snow Telemetry (SNOTEL) network, is needed to verify both the utility of the snow drought classification methodology and the nonlinear relationship between warm snow drought risk and mean winter temperature. Further, the Livneh et al. (2015) gridded hydrometeorological data set used in this study was created using meteorological stations that do not span the full temporal period, and thus, the data set is not suitable for trend analysis. While the documented relationship between warm snow drought risk and T_w (Figure 4b) suggests that temperature-related snow drought risk is likely to increase with continued climate warming, further study with data sets appropriate for trend analysis, like the SNOTEL network, are needed to confirm the insights provided by this model-based analysis.

Additional limitations of this study are related to the region-wide piecewise linear regression analysis, which is equivalent to a space-for-time substitution and relies on the logic that a warmer future may look like historically warmer places do now (Luce et al., 2014). A potential concern regarding this method is that different geographic locations may not share the same weather sequences or seasonal timing of precipitation. These geographical variations likely explain some of the residual variance within the piecewise linear regression model presented in Figure 4b. To further analyze the utility of this space-for-time substitution, relationships between warm snow drought risk and T_w were investigated at the ecoregion scale, revealing that the positive nonlinear relationship shown in Figure 4b is present in all 15 ecoregions; however, the ecoregion-based regression slopes exhibit some variability (Figure S3 and Table S6). The Blue Mountains, for example, exhibits a substantially higher slope between the −3.1 and 1.4 °C breakpoints (i.e., S2 in Table S6) while the North Cascades regression slope is lower than the region-wide slope in this interval, suggesting that compared to the region-wide average, the Blue Mountains exhibits slightly higher sensitivity to increases in T_w while the North Cascades exhibit slightly lower sensitivity. Based on the strong positive correlation between warm snow drought risk and T_w in all ecoregions (Figure S3), it is clear that temperature drives elevated snow drought risk. Solar radiation and humidity are also important (Harpold & Brooks, 2018; Musselman et al., 2017), and further research is needed to understand the causal mechanisms behind the variation in regression slopes (Table S6). Combining the snow drought classification methodology presented in this study with direct warming experiments using VIC and/or other appropriate physically based hydrological models would have value for further understanding of snow drought risk in the context of a warming climate.

A further limitation of the piecewise linear regression analysis is that it may identify breakpoints in the presence of any nonlinearity, even if that nonlinearity is smooth and contains no discrete breakpoints. Thus, interpretation of the temperature thresholds in terms physical hydrological processes is crucial to assessing the meaningfulness of this study and for defining future research directions. It is important to note, therefore, that the presence of these temperature thresholds is likely related to the relationship between T_w

and precipitation phase and the energy available for melt. For locations where T_w is above the temperature threshold of −3.1 °C, the rain-snow transition is within the range of interannual variability in daily temperatures. Thus, warm years result in more rain and less snow and/or midseason/early spring melt events. Below the −3.1 °C temperature threshold, warm years are less likely to have these impacts. For locations where T_w is above the 1.4 °C threshold, much of the snow season has daily temperatures near the rain-snow transition, and, as documented by previous studies (Adam et al., 2009; Brown & Mote, 2009; Luce et al., 2014; Mote et al., 2018), even small temperature anomalies can have large impacts on peak SWE in these locations. Further, the impact of temperature on normalized peak SWE is amplified in these relatively warm locations (i.e., $T_w > 1.4$ °C) because the snowpacks are smaller and take less energy to melt. This physical basis provides confidence in the chosen methodology and outcomes and guidance for future studies. However, additional studies, using artificial neural networks or information theoretic polynomial selection (Cannon, 2018; Fleming, 2007; Fleming & Dahlke, 2014), for example, may provide additional insights into the relationship between T_w and snow drought risk.

This study presented a novel approach to snow drought classification and to the quantification of SWE *T*-sensitivity. While the grid-cell-based winter season definition using thawing degrees (TD) and precipitation (*P*) as the predictor variables exhibited the greatest predictive ability for peak SWE, the gains in R^2 values were not large (+0.03 R^2 domain wide; Table S2) compared to the other, simpler methods (i.e., T_w, *P* with 1 November to 1 April winter season). Thus, it could be argued that the simpler method should be used. Previous work (Dierauer et al., 2018) using observed streamflow data from mountain catchments in WNA, however, showed that runoff and low flows are more sensitive to TD than T_w. As the duration and severity of low flow periods are highly dependent on snowmelt hydrology in mountain catchments, the observations of Dierauer et al. (2018) suggest that snow accumulation and melt are also more sensitive to TD than to T_w. Additionally, SWE *T*-sensitivities estimated from the grid-cell-based approach using TD and *P* as the predictors were higher than the other methods in the warmer, maritime ecoregions (Table S3) and standard error estimates were lower (Table S4), supporting the use of the more complicated methodology and suggesting *T*-sensitivity may be underestimated in the warmer maritime regions using the more conventional methods.

5. Conclusions

This study provides new detailed insight into the spatial and ecoregion differences in snow drought regimes across the snow-dominated regions of the western United States and southwestern Canada. The relationships between mean winter temperature, snow drought risk, and SWE sensitivity demonstrate that temperature thresholds exist, above which warm snow drought risk and SWE *T*-sensitivity increase at a greater rate. While previous studies have shown that the *T*-sensitivity of SWE tends to decrease with elevation and increase with mean winter temperatures, the *acceleration* in hydroclimatic change at distinct temperature thresholds has not been demonstrated before. Identified temperature thresholds at T_w values of −3.1 and 1.4 °C were used to map temperature-related snow drought susceptibility, revealing that 3% of the volume of the nonglaciated snowpack in snow-dominated regions of the western United States and southwestern Canada is highly susceptible to warm snow droughts and an additional 24% exhibits medium susceptibility. The susceptibility mapping presented in this study is a first step toward a snow drought risk assessment in the context of a nonstationary climate and can be transferred to other mountainous regions and used to inform snow drought mitigation strategies and water resource management planning.

Acknowledgments
This research was supported by the Pacific Institute for Climate Solutions and a Simon Fraser University graduate entrance scholarship to Jennifer Dierauer. The gridded hydrometeorological data are documented in Livneh et al. (2015). The main data sets created from this study, including snow drought risk and the temperature-related snow drought susceptibility, are available in raster (.asc) format (https://doi.org/10.6084/m9.figshare.7767212).

References

Adam, J. C., Hamlet, A. F., & Lettenmaier, D. P. (2009). Implications of global climate change for snowmelt hydrology in the twenty-first century. *Hydrological Processes*, *23*(7), 962–972. https://doi.org/10.1002/hyp.7201

Ajami, H., Meixner, T., Dominguez, F., Hogan, J., & Maddock, T. (2012). Seasonalizing mountain system recharge in semi-arid basins—Climate change impacts. *Groundwater*, *50*(4), 585–597. https://doi.org/10.1111/j.1745-6584.2011.00881.x

Alexander, M. A., Scott, J. D., Swales, D., Hughes, M., Mahoney, K., & Smith, C. A. (2015). Moisture pathways into the U.S. Intermountain West associated with heavy precipitation events. *Journal of Hydrometeorology*, *16*(3), 1184–1206. https://doi.org/10.1175/JHM-D-14-0139.1

Alexander, P., Brekke, L., Davis, G., Gangopadhyay, S., Grantz, K., Hennig, C. et al. (2011). Reclamation, SECURE Water Act Section 9503(c)—Reclamation climate change and water, Report to Congress, 2011. Bureau of Reclamation, U.S. Department of Interior.

Allamano, P., Claps, P., & Laio, F. (2009). Global warming increases flood risk in mountainous areas. *Geophysical Research Letters*, *36*, L24404. https://doi.org/10.1029/2009GL041395

Bales, R. C., Goulden, M. L., Hunsaker, C. T., Conklin, M. H., Hartsough, P. C., O'Geen, A. T., et al. (2018). Mechanisms controlling the impact of multi-year drought on mountain hydrology. *Scientific Reports*, *8*(1), 690. https://doi.org/10.1038/s41598-017-19007-0

Balsamo, G., Albergel, C., Beljaars, A., Boussetta, S., Brun, E., Cloke, H., et al. (2015). ERA-Interim/Land: A global land surface reanalysis dataset. *Hydrology and Earth System Sciences*, *19*(1), 389–407. https://doi.org/10.5194/hess-19-389-2015

Barnett, T. P., Adam, J. C., & Lettenmaier, D. P. (2005). Potential impacts of a warming climate on water availability in snow-dominated regions. *Nature*, *438*(7066), 303–309. https://doi.org/10.1038/nature04141

Barnett, T. P., Pierce, D. W., Hidalgo, H. G., Bonfils, C., Santer, B. D., Das, T., et al. (2008). Human-induced changes in the hydrology of the western United States. *Science*, *319*(5866), 1080–1083. https://doi.org/10.1126/science.1152538

Barnhart, T. B., Molotch, N. P., Livneh, B., Harpold, A. A., Knowles, J. F., & Schneider, D. (2016). Snowmelt rate dictates streamflow. *Geophysical Research Letters*, *43*, 8006–8016. https://doi.org/10.1002/2016GL069690

Berghuijs, W. R., Woods, R. A., & Hrachowitz, M. (2014). A precipitation shift from snow towards rain leads to a decrease in streamflow. *Nature Climate Change*, *4*(7), 583–586. https://doi.org/10.1038/nclimate2246

Brown, R. D., & Mote, P. W. (2009). The response of Northern Hemisphere snow cover to a changing climate. *Journal of Climate*, *22*(8), 2124–2145. https://doi.org/10.1175/2008JCLI2665.1

Cannon, A. J. (2005). Defining climatological seasons using radially constrained clustering. *Geophysical Research Letters*, *32*, L14706. https://doi.org/10.1029/2005GL023410

Cannon, A. J. (2018). Non-crossing nonlinear regression quantiles by monotone composite quantile regression neural network, with application to rainfall extremes. *Stochastic Environmental Research and Risk Assessment*, *32*(11), 3207–3225. https://doi.org/10.1007/s00477-018-1573-6

Cayan, D. R., Redmond, K. T., & Riddle, L. G. (1999). ENSO and hydrologic extremes in the western United States. *Journal of Climate*, *12*(9), 2881–2893. https://doi.org/10.1175/1520-0442(1999)012<2881:EAHEIT>2.0.CO;2

Cherkauer, K. A., Bowling, L. C., & Lettenmaier, D. P. (2003). Variable infiltration capacity cold land process model updates. *Global and Planetary Change*, *38*(1–2), 151–159. https://doi.org/10.1016/S0921-8181(03)00025-0

Cline, D. W. (1997). Snow surface energy exchanges and snowmelt at a continental, midlatitude Alpine site. *Water Resources Research*, *33*(4), 689–701. https://doi.org/10.1029/97WR00026

Commission for Environmental Cooperation. (2011). North American Terrestrial Ecoregions—Level III, Commission for Environmental Cooperation, Montreal, Canada.

Cooper, M. G., Nolin, A. W., & Safeeq, M. (2016). Testing the recent snow drought as an analog for climate warming sensitivity of Cascades snowpacks. *Environmental Research Letters*, *11*(8), 084009. https://doi.org/10.1088/1748-9326/aa/8/084009

Dai, Y., Zeng, X., Dickinson, R. E., Baker, I., Bonan, G. B., Bosilovich, M. G., et al. (2003). The common land model. *Bulletin of the American Meteorological Society*, *84*(8), 1013–1024. https://doi.org/10.1175/BAMS-84-8-1013

Davies, R. B. (1987). Hypothesis testing when a nuisance parameter is present only under the alternative. *Biometrika*, *74*, 33–43.

Déry, S. J., Stahl, K., Moore, R. D., Whitfield, P. H., Menounos, B., & Burford, J. E. (2009). Detection of runoff timing changes in pluvial, nival, and glacial rivers of western Canada. *Water Resources Research*, *45*, W04426. https://doi.org/10.1029/2008WR006975

Dierauer, J. R., Whitfield, P. H., & Allen, D. M. (2018). Climate controls on runoff and low flows in mountain catchments of western North America. *Water Resources Research*, *54*, 7495–7510. https://doi.org/10.1029/2018WR023087

Earman, S., Campbell, A. R., Phillips, F. M., & Newman, B. D. (2006). Isotopic exchange between snow and atmospheric water vapor: Estimation of the snowmelt component of groundwater recharge in the southwestern United States. *Journal of Geophysical Research*, *111*, D09302. https://doi.org/10.1029/2005JD006470

Feng, X., Sahoo, A., Arsenault, K., Houser, P., Luo, Y., & Troy, T. J. (2008). The impact of snow model complexity at three CLPX sites. *Journal of Hydrometeorology*, *9*(6), 1464–1481. https://doi.org/10.1175/2008JHM860.1

Fleming, S. W. (2007). Artificial neural network forecasting of nonlinear Markov processes. *Canadian Journal of Physics*, *85*(3), 279–294. https://doi.org/10.1139/p07-037

Fleming, S. W., & Dahlke, H. E. (2014). Parabolic northern-hemisphere river flow teleconnections to El Niño-Southern Oscillation and the Arctic Oscillation. *Environmental Research Letters*, *9*(10). https://doi.org/10.1088/1748-9326/9/10/104007

Fleming, S. W., Whitfield, P. H., Moore, R. D., & Quilty, E. J. (2007). Regime-dependent streamflow sensitivities to Pacific climate modes cross the Georgia-Puget transboundary ecoregion. *Hydrological Processes*, *21*(24), 3264–3287. https://doi.org/10.1002/hyp.6544

Groisman, P. Y., Knight, R. W., Karl, T. R., Easterling, D. R., Sun, B., & Lawrimore, J. H. (2004). Contemporary changes of the hydrological cycle over the contiguous United States: Trends derived from in situ observations. *Journal of Hydrometeorology*, *5*(1), 64–85. https://doi.org/10.1175/1525-7541(2004)005<0064:CCOTHC>2.0.CO;2

Guan, B., Molotch, N. P., Waliser, D. E., Fetzer, E. J., & Neiman, P. J. (2013). The 2010/2011 snow season in California's Sierra Nevada: Role of atmospheric rivers and modes of large-scale variability. *Water Resources Research*, *49*, 6731–6743. https://doi.org/10.1002/wrcr.20537

Harpold, A., Brooks, P., Rajagopal, S., Heidbuchel, I., Jardine, A., & Stielstra, C. (2012). Changes in snowpack accumulation and ablation in the Intermountain West. *Water Resources Research*, *48*, W11501. https://doi.org/10.1029/2012WR011949

Harpold, A. A. (2016). Diverging sensitivity of soil water stress to changing snowmelt timing in the western US. *Advances in Water Resources*, *92*, 116–129. https://doi.org/10.1016/j.advwatres.2016.03.017

Harpold, A. A., & Brooks, P. D. (2018). Humidity determines snowpack ablation under a warming climate. *Proceedings of the National Academy of Sciences*, *115*(6), 1215–1220. https://doi.org/10.2073/pnas.1716789115

Harpold, A. A., Dettinger, M., & Rajagopal, S. (2017). Defining snow drought and why it matters. *Eos Transactions American Geophysical Union*, 98. https://doi.org/10.1029/2017EO068775

Harpold, A. A., & Kohler, M. (2017). Potential for changing extreme snowmelt and rainfall events in the mountains of western North America. *Journal of Geophysical Research: Atmospheres*, *122*, 13,219–13,228. https://doi.org/10.1002/2017JD027704

Hatcher, K. L., & Jones, J. A. (2013). Climate and streamflow trends in the Columbia River Basin: Evidence for ecological and engineering resilience to climate change. *Atmosphere-Ocean*, *51*(4), 436–455. https://doi.org/10.1080/07055900.2013.808167

Hatchett, B. J., & McEvoy, D. J. (2018). Exploring the origins of snow drought in the northern Sierra Nevada, California. *Earth Interactions*, *22*(2), 1–13. https://doi.org/10.1175/EI-D-17-0027.1

Howitt, R., MacEwan, D., Medellín-Azuara, J., Lund, J., &Sumner, D. (2015). Economic analysis of the 2015 drought for California agriculture. UC Davis Center for Watershed Sciences.Retrieved March 2018 fromhttps://watershed.ucdavis.edu/files/biblio/Final_Drought%20Report_08182015_Full_Report_WithAppendices.pdf

Hu, J., Moore, D. J. P., Burns, S. P., & Monson, R. K. (2010). Longer growing seasons lead to less carbon sequestration by a subalpine forest. *Global Change Biology*, *16*(2), 771–783. https://doi.org/10.1111/j.1365-2486.2009.01967.x

Jaeger, W. K., Amos, A., Bigelow, D. P., Chang, H., Conklin, D. R., Haggerty, R., et al. (2017). Finding water scarcity amid abundance using human-natural system models. *Proceedings of the National Academy of Sciences*, *114*(45), 11884–11889. https://doi.org/10.1073/pnas.1706847114

Jenicek, M., Seibert, J., Zappa, M., Staudinger, M., & Jonas, J. (2016). Importance of maximum snow accumulation for summer low flows in humid catchments. *Hydrology and Earth System Sciences*, *20*(2), 859–874. https://doi.org/10.5194/hess-20-859-2016

Jordan, R.E. (1991). A one-dimensional temperature model for a snow cover: Technical documentation for SNTHERM.89. CRREL Special Rep. 91-16, Cold Regions Research and Engineering Laboratory, 61 pp.

Kapnick, S., & Hall, A. (2012). Causes of recent changes in western North American snowpack. *Climate Dynamics*, *38*(9–10), 1885–1899. https://doi.org/10.1007/s00382-011-1089-y

Leith, R. M. M., & Whitfield, P. H. (1998). Evidence of climate change effects on hydrology of streams in south-central BC. *Canadian Water Resources Journal*, *23*(3), 219–230. https://doi.org/10.4296/cwrj2303219

Li, D., Wrzesien, M. L., Durand, M., Adam, J., & Lettenmaier, D. P. (2017). How much runoff originates as snow in the western United States, and how will that change in the future? *Geophysical Research Letters*, *44*, 6163–6172. https://doi.org/10.1002/2017GL073551

Liang, X., Lettenmaier, D. P., Wood, E. F., & Burges, S. J. (1994). A simple hydrologically based model of land surface water and energy fluxes for general circulation models. *Journal of Geophysical Research*, *99*(D7), 14415–14,428. https://doi.org/10.1029/94JD00483

Livneh, B., Bohn, T. J., Pierce, D. W., Munoz-Arriola, F., Nijssen, B., Vose, R., et al. (2015). A spatially comprehensive, hydrometeorological data set for Mexico, the U.S., and Southern Canada 1950-2013. *Scientific Data*, *2*, 150042. https://doi.org/10.1038/sdata.2015.42

Livneh, B., Rosenberg, E. A., Lin, C., Nijssen, B., Mishra, M., Andreadis, K. M., et al. (2013). A long-term hydrologically based dataset of land surface fluxes and states for the conterminous United States: Update and extensions. *Journal of Climate*, *26*(23), 9384–9392. https://doi.org/10.1175/JCLI-D-12-00508.1

Luce, C. H., Lopez-Burgos, V., & Holden, Z. (2014). Sensitivity of snowpack storage to precipitation and temperature using spatial and temporal analog models. *Water Resources Research*, *50*, 9447–9462. https://doi.org/10.1002/2013WR014844

Ludlum, D. M. (1978). The snowfall season of 1976. *Weatherwise*, *31*(1), 20–46. https://doi.org/10.1080/00431672.1978.9931847

Male, D. H., & Granger, R. J. (1981). Snow surface energy exchange. *Water Resources Research*, *17*(3), 609–627. https://doi.org/10.1029/WR017i003p00609

Moore, R. D., Fleming, S. W., Menounos, B., Wheate, R., Fountain, A., Stahl, K., et al. (2009). Glacier change in western North America: Influences on hydrology, geomorphic hazards and water quality. *Hydrological Processes*, *23*(1), 42–61. https://doi.org/10.1002/hyp.7162

Morán-Tejeda, E., López-Moreno, J. I., & Beniston, M. (2013). The changing roles of temperature and precipitation on snowpack variability in Switzerland as a function of altitude. *Geophysical Research Letters*, *40*, 2131–2136. https://doi.org/10.1002/grl.50463

Mote, P. W. (2003). Trends in snow water equivalent in the Pacific Northwest and their climatic causes. *Geophysical Research Letters*, *30*(12), 1601. https://doi.org/10.1029/2003GL017258

Mote, P. W. (2006). Climate-driven variability and trends in mountain snowpack in western North America. *Journal of Climate*, *19*(23), 6209–6220. https://doi.org/10.1175/JCLI3971.1

Mote, P. W., Hamlet, A. F., Clark, M. P., & Lettenmaier, D. P. (2005). Declining mountain snowpack in western North America. *Bulletin of the American Meteorological Society*, *86*(1), 39–50. https://doi.org/10.1175/BAMS-86-1-39

Mote, P. W., Li, S., Lettenmaier, D. P., Xiao, M., & Engel, R. (2018). Dramatic declines in snowpack in the western US. *Climate and Atmospheric Science*, *1*(1), 1–6. https://doi.org/10.1038/s41612-018-0012-1

Mote, P. W., Rupp, D. E., Li, S., Sharp, D. J., Otto, F., Uhe, P. F., et al. (2016). Perspectives on the causes of exceptionally low 2015 snowpack in the western United States. *Geophysical Research Letters*, *43*, 10,980–10,988. https://doi.org/10.1002/2016GL069965

Muggeo, V. M. R. (2008). Segmented: An R package to fit regression models with broken-line relationships. *R News*, *8*(1), 20–25.

Musselman, K. N., Clark, M. P., Liu, C., Kyoko, I., & Rasmussen, R. (2017). Slower snowmelt in a warmer world. *Nature Climate Change*, *7*(3), 214–219. https://doi.org/10.1038/NCLIMATE3225

Nolin, A. W., & Daly, C. (2006). Mapping "at risk" snow in the Pacific Northwest. *Journal of Hydrometeorology*, *7*(5), 1164–1171. https://doi.org/10.1175/JHM543.1

O'Neel, S., Hood, E., Arendt, A., & Sass, L. (2014). Assessing streamflow sensitivity to variations in glacier mass balance. *Climatic Change*, *123*(2), 329–341. https://doi.org/10.1007/s10584-013-1042-7

Painter, T. H., Berisford, D. F., Boardman, J. W., Bormann, K. J., Deems, J. S., Gehrke, F., et al. (2016). The Airborne Snow Observatory: Fusion of scanning lidar, imaging spectrometer, and physically-based modeling for mapping snow water equivalent and snow albedo. *Remote Sensing of Environment*, *184*, 139–152. https://doi.org/10.1016/j.rse.2016.06.018

Pederson, G. T., Gray, S. T., Ault, T., Marsh, W., Fagre, D. B., Bunn, A. G., et al. (2011). Climate controls on snowmelt hydrology of the Northern Rocky Mountains. *Journal of Climate*, *24*(6), 1666–1687. https://doi.org/10.1175/2010JCLI3729.1

Pfeffer, W. T., Arendt, A. A., Bliss, A., Bolch, T., Cogley, J. G., Gardner, A. S., et al., & The Randolph Consortium (2014). The Randolph Glacier Inventory: A globally complete inventory of glaciers. *Journal of Glaciology*, *60*, 221. https://doi.org/10.3189/2014JoG12J176

Pulliainen, J. (2006). Mapping of snow water equivalent and snow depth in boreal and sub-arctic zones by assimilating space-borne microwave radiometer data and ground-based observations. *Remote Sensing of Environment*, *101*(2), 257–269. https://doi.org/10.1016/j.rse.2006.01.002

Randolph Glacier Inventory Consortium. (2017). Randolph glacier inventory (RGI)—A dataset of global glacier outlines: Version 6.0. Global Land Ice Measurements from Space, Boulder. https://doi.org/10.72625/N5-RGI60

Regonda, S. K., Rajagopalan, B., Clark, M., & Pitlick, J. (2005). Seasonal cycle shifts in hydroclimatology over the western U.S. *Journal of Climate*, *18*(2), 372–384. https://doi.org/10.1175/JCLI-3272.1

Rodell, M., Houser, P. R., Jambor, U., Gottschalck, J., Mitchell, K., Meng, C.-J., et al. (2004). The global land data assimilation system. *Bulletin of the American Meteorological Society*, *85*(3), 381–394. https://doi.org/10.1175/BAMS-85-3-381

Rood, S. B., Foster, S. G., Hillman, E. J., Luek, A., & Zanewich, K. P. (2016). Flood moderation: Declining peak flows along some Rocky Mountain rivers and the underlying mechanism. *Journal of Hydrology*, *536*, 174–182. https://doi.org/10.1016/j.jhydrolo.2016.02.043

Safeeq, M., Shukla, S., Arismendi, I., Grant, G. E., Lewis, S. L., & Nolin, A. (2016). Influence of winter season climate variability on snow-precipitation ratio in the western United States. *International Journal of Climatology*, *36*(9), 3175–3190. https://doi.org/10.1002/joc.4545

Scalzitti, J., Strong, C., & Kochanski, A. (2016). Climate change impact on the roles of temperature and precipitation in western U.S. snowpack variability. *Geophysical Research Letters*, *43*, 5361–5369. https://doi.org/10.1002/2016GL068798

Seager, R., Ting, M., Li, C., Naik, N., Cook, B., Nakamura, J., & Liu, H. (2013). Projections of declining surface-water availability for the southwestern United States. *Nature Climate Change*, *3*(5), 482–486. https://doi.org/10.1038/NCLIMATE1787

Seber, G. A. (2015). Nonlinear regression models. In *The linear model and hypothesis* (pp. 117–128). Cham: Springer. https://doi.org/10.1007/978-3-319-21930-1_8

Sellers, W. D. (1968). Climatology of monthly precipitation patterns in the western United States, 1931-1966. *Monthly Weather Review*, *96*(9), 585–595. https://doi.org/10.1175/1520-0493(1968)096<0585:COMPPI>2.0.CO;2

Snauffer, A. M., Hsieh, W. W., Cannon, A. J., & Schnorbus, M. A. (2018). Improving gridded snow water equivalent products in British Columbia, Canada: Multi-source data fusion by neural network models. *The Cryosphere*, *12*(3), 891–905. https://doi.org/10.5194/tc-12-891-2018

Sospedra-Alfonso, R., Melton, J. R., & Merryfield, W. J. (2015). Effects of temperature and precipitation on snowpack variability in the Central Rocky Mountains as a function of elevation. *Geophysical Research Letters*, *42*, 4429–4438. https://doi.org/10.1002/2015GL063898

Sospedra-Alfonso, R., & Merryfield, W. J. (2017). Influences of temperature and precipitation on historical and future snowpack variability over the Northern Hemisphere in the second generation Canadian Earth System Model. *Journal of Climate*, *30*(12), 4633–4656. https://doi.org/10.1175/JCLI-D-16-0612.s1

Sproles, E. A., Roth, T. R., & Nolin, A. W. (2017). Future snow? A spatial-probabilistic assessment of the extraordinarily low snowpacks of 2014 and 2015 in the Oregon Cascades. *The Cryosphere*, *11*(1), 331–341. https://doi.org/10.5194/tc-11-331-2017

Swales, D., Alexander, M., & Hughes, M. (2016). Examining moisture pathways and extreme precipitation in the U.S. Intermountain West using self-organizing maps. *Geophysical Research Letters*, *43*, 1727–1735. https://doi.org/10.1002/2015GL067478

Verdon-Kidd, D. C., & Kiem, A. S. (2010). Quantifying drought risk in a nonstationary climate. *Journal of Hydrometeorology*, *11*(4), 1019–1031. https://doi.org/10.1175/2010JHM1215.1

Westerling, A. L., Hidalgo, H. G., Cayan, D. R., & Swetnam, T. W. (2006). Warming and earlier spring increase western U.S. forest wildfire activity. *Science*, *313*(5789), 940–943. https://doi.org/10.1126/science.1128834

Whitfield, P. H., & Cannon, A. J. (2000). Recent variations in climate and hydrology in Canada. *Canadian Water Resources Journal*, *25*(1), 19–65. https://doi.org/10.4296/cwrj2501019

Wiesnet, D. (1981). Winter snow drought. *Eos, Transactions of the American Geophysical Union*, *62*(14), 137–137. https://doi.org/10.1029/EO062i014p00137-04

Winchell, T. S., Barnard, D. M., Monson, R. K., Burns, S. P., & Molotch, N. P. (2016). Earlier snowmelt reduces atmospheric carbon uptake in midlatitude subalpine forests. *Geophysical Research Letters*, *43*, 8160–8168. https://doi.org/10.1002/2016GL069769

Winograd, I. J., Riggs, A. C., & Coplen, T. B. (1998). The relative contributions of summer and cool-season precipitation to groundwater recharge, Spring Mountains, Nevada, USA. *Hydrogeology Journal*, *6*(1), 77–93. https://doi.org/10.1007/s100400050135

Wrzesien, M. L., Durand, M. T., Pavelsky, T. M., Kapnick, S. B., Zhang, Y., Guo, J., & Shun, C. K. (2018). A new estimate of North American mountain snow accumulation from regional climate model simulations. *Geophysical Research Letters*, *45*, 1423–1432. https://doi.org/10.1002/2017GL076664